Science of the Total Environment 951 (2024) 175365

Contents lists available at ScienceDirect

Science of the Total Environment

journal homepage: www.elsevier.com/locate/scitotenv

Climate change accelerates water and biogeochemical cycles in temperate agricultural catchments

M.Z. Bieroza [a,*], L. Hallberg [a], J. Livsey [a], M. Wynants [a,b]

[a] Department of Soil and Environment, Swedish University of Agricultural Sciences, Box 7014, 75007 Uppsala, Sweden
[b] Isotope Bioscience Laboratory - ISOFYS, Department of Green Chemistry and Technology, Ghent University, Coupure Links 653, 9000 Gent, Belgium

HIGHLIGHTS

- We modelled effects of climate change in two agricultural catchments.
- Wetter and drier conditions will activate rapid and flashy delivery flow pathways.
- Concurrent increases in solute/sediment mobilisation will deteriorate water quality.
- The negative effects on water quality will be consistent in varied catchments.
- Strategic planning and implementation of mitigation measures will be needed.

GRAPHICAL ABSTRACT

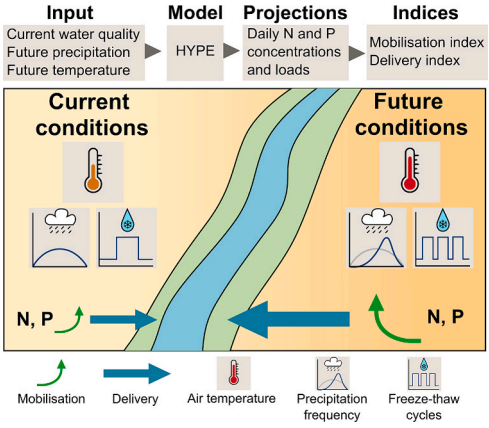

ARTICLE INFO

Editor: Ouyang Wei

Keywords:
Water quality
Droughts and floods
Climatic predictions
Concentrations and loads
Concentration-discharge relationships

ABSTRACT

Climate change is expected to significantly deteriorate water quality in heavily managed agricultural landscapes, however, the exact mechanisms of these impacts are unknown. In this study we adopted a modelling approach to predict the multiple effects of climate change on hydrological and biogeochemical responses for dominant solutes and particulates in two agriculture-dominated temperate headwater catchments. We used climatic projections from three climatic models to simulate future flows, mobilisation and delivery of solutes and particulates. This allowed an examination of potential drivers by identifying changes in flow pathway distribution and key environmental variables. We found that future climate conditions will lead to a general increase in stream discharge as well as higher concentrations and loads of solutes and particulates. However, unlike previous studies, we observed a higher magnitude of change during the warmer part of the year. These changes will reduce the relative importance of winter flows on solute and particulate transport, leading to both higher and more evenly distributed concentrations and loads between seasons. We linked these changes to the higher importance of superficial flow pathways of tile and surface runoff driven by more rapid transition from extremely wet to dry conditions. Overall, the observed increase in solute and particulate mobilisation and delivery will lead to

* Corresponding author.
E-mail address: magdalena.bieroza@slu.se (M.Z. Bieroza).

https://doi.org/10.1016/j.scitotenv.2024.175365
Received 9 May 2024; Received in revised form 24 July 2024; Accepted 5 August 2024
Available online 6 August 2024

widespread water quality deterioration. Mitigation of this deterioration would require adequate management efforts to address the direct and indirect negative effects on stream biota and water scarcity.

1. Introduction

Climate change has increased the likelihood and frequency of extreme hydrological events, such as floods and drought, according to both predictive models and hydrological observations from around the world (Payne et al., 2020). In human impacted landscapes, where water buffering capacity is significantly reduced, the effects of climate change on hydrological response will be amplified, with both flood and drought events becoming more frequent, severe, and unpredictable. Agricultural temperate catchments in Europe and Northern America that sustain intensive food production will be particularly sensitive to these negative changes. This sensitivity results from major anthropogenic impacts in agricultural catchments including artificial drainage and channel straightening (Blann et al., 2009) and legacy nutrients leading to eutrophication and hypoxia (Basu et al., 2022; Bol et al., 2018). However, the effects of climate change on the hydrological cycle within agricultural temperate catchments will likely vary between the warmer temperate (Mediterranean and oceanic) and colder continental and boreal climates. In colder continental climates as in southern Sweden, increased precipitation, reduced spring snowmelt and more frequent droughts and freeze and thaw cycles (Grusson et al., 2021) will shift agricultural streams towards more flashy hydrological regimes. This shift will have generally unknown effects on water quality and stream ecology (Li et al., 2024; van Vliet et al., 2023).

Most of the existing research focuses on the water quality effects for individual drought or flood events (Li et al., 2024), with limited understanding of their successive effects on seasonal to multidecadal time scales. Several empirical studies show that prolonged hydrological drought, resulting in stream dry out, reduces mobilisation and delivery of nutrients and sediments. This occurs due to the disconnection of the hydrological units, between the stream and catchment and riparian sources (Outram et al., 2016; Van Loon et al., 2019). The surface and shallow subsurface flow pathways are the first to stop under drought conditions while groundwater delivery can persist longer. Therefore, the effect of drought on water quality depends mostly on the relative solute and particulate concentrations in these different flow end-members (Stewart et al., 2022). If solute and sediment delivery is dominated by distal diffuse catchment sources, then there is a reduction in their stream concentrations under drought conditions. Similar patterns occur if their sources are located within the stream e.g., from resuspension of in-stream sediments (Mosley, 2015). In catchments dominated by legacy sources from past fertilisation (Basu et al., 2022) or point sources with delivery along groundwater flow pathways, the in-stream solute concentrations during drought are usually high. This is due to significantly reduced dilution capacity (Whitehead et al., 2009). During droughts, terrestrial vegetation becomes water limited, decreasing the uptake of nutrients, leading to their build-up in the soil. Moreover, the oxygenation of previously submerged channel beds and wet areas suppresses nitrogen removal by denitrification (Gómez et al., 2011) but also stimulates the mineralisation of nutrients from the organic and particulate forms. The period of hydrological reconnection after prolonged drought leads therefore to rapid mobilisation of solutes and sediments accumulated in soils, the riparian zone and within stream channels (Li et al., 2024). Thus, the first storm event after prolonged drought typically results in much higher concentrations of solutes and particulates. These elevated levels gradually decrease as stream and the catchment become hydrologically reconnected (Bieroza et al., 2019; Mosley, 2015).

The effects of floods on water quality are well documented owing to increasing availability of high-frequency discharge and solute/sediment measurements. These measurements have enabled the establishing of concentration-discharge relationships. Studies show that stream water quality is driven by seasonally changing hydrological connectivity between in-stream and distal catchment sources (Mellander et al., 2022; Stewart et al., 2022). During periods of high precipitation and high hydrological connectivity (typically winters in the northern hemisphere), high magnitude storm events lead to the highest observed concentrations and loads of solutes and sediments. These events are driven by rapid mobilisation and delivery of solutes and sediments from diffuse and in-stream sources with typically clockwise concentration-discharge (C-Q) patterns and chemostatic responses (Bieroza et al., 2023; Godsey et al., 2019; Knapp et al., 2022). During summers, the importance of distal catchment sources diminishes due to reduced hydrological connectivity and in-stream sediment resuspension whereby solute delivery from riparian sources dominates. During summer flow events, there is usually a delayed mobilisation and delivery of solutes and sediments with predominantly anticlockwise C-Q patterns and chemodynamic responses, indicating transport-limitation (Bieroza and Heathwaite, 2015; Winter et al., 2021). The onset of summer flood events can be rapid due to intensive convective precipitation. As a result, there is generally a larger variation in summer mobilisation/delivery and C-Q patterns compared to more uniform winter patterns driven by frontal precipitation (Mellander et al., 2018).

There is relatively good mechanistic understanding of solute and sediment mobilisation and delivery on the short-term temporal time scales, from individual storm events to seasons. This is not, however, well conceptualised for future climatic conditions (Li et al., 2024; van Vliet et al., 2023). Previous studies suggest that complex feedbacks between changing temperature regimes and precipitation patterns, together with uncertainties in climate predictions (Payne et al., 2020) propagate into water quality responses that are challenging to predict (Li et al., 2024; Whitehead et al., 2009). For example, in continental temperate climates, the mobilisation and delivery of nutrients is expected to shift from spring snowmelt to high-intensity precipitation events during summer and autumn (Liu et al., 2019). In oceanic temperate climates, winter mobilisation and delivery will prevail and intensify, resulting in a greater need for mitigation and remediation interventions to offset these negative impacts (Ockenden et al., 2017). Recently, Mellander et al. (2022) suggested a framework to assess the variation in phosphorus mobilisation and delivery to streams using integrated climate-chemical indices based on high-frequency water quality data (Mellander et al., 2018). This recent body of research on C-Q metrics, mobilisation and delivery indicators and catchment modelling provides opportunities for improved conceptualisation and testing of future climatic effects on water quality across temporal scales from seasons to decades.

In this paper we combine high-frequency data analysis with climatic and hydrochemical modelling for two agricultural catchments in Sweden to establish current and future mobilisation and delivery patterns for solutes (nitrate-nitrogen [NO_3-N] and soluble reactive phosphorus [SRP]) and particulates (particulate phosphorus [PP] and suspended sediments [SS]). We cross-reference these patterns with the underlying catchment properties and in-stream processes such as nutrient mineralisation, crop uptake and denitrification to gain a better mechanistic understanding of driver dependencies. We hypothesize that a higher frequency of extreme hydrological events leads to water quality deterioration by increasing the concentration and load of solutes and particulates in streams. We also expect these negative effects to be similar in varied agricultural catchments.

2. Materials and methods

2.1. Hydrochemical data and catchments' characteristics

The study was conducted in two agriculturally-dominated catchments, Tullstorp and Hestad (Supporting Fig. 1). These catchments vary in size, cropping regimes, climatic and soil characteristics and hydrology. Both catchments represent the dominant crop-growing regions in Sweden, with extensive tile drainage of soils. The Hestad catchment is located in central east Sweden and drains clay loam soils (Bieroza et al., 2019), and the Tullstorp catchment is located in the coastal zone of south Sweden, draining loam soils. The Tullstorp catchment is larger (62.1 km^2), but also has a higher percentage of arable land, dominated by autumn- and spring-sown cereal crops (57 % and 8 % respectively), together with pasture and root crops (8.3 %) (Wynants et al., 2024). The Hestad catchment (7.6 km^2) is dominated by autumn-sown cereal crops (54.7 %) but also includes forest (25.5 %) and pasture (16.9 %). Tullstorp has an oceanic temperate climate (Cfb, according to the Köppen-Geiger classification) with average annual precipitation of 790 mm, and an average temperature of 8.7 °C. In contrast, Hestad has a continental temperate climate (Dfb) with average annual precipitation of 580 mm and average temperature of 7.9 °C. Tullstorp is both warmer and wetter than Hestad.

Water flow and quality have been continuously monitored at Hestad and Tullstorp since 1988 and 2009 respectively. The Hestad catchment is gauged continuously for discharge at 15 min time steps using a small basin with V-notch at the outlet (Bieroza et al., 2019) and using stage sensors along the stream network (Hallberg et al., 2024a). Water quality sampling in Hestad catchment includes continuous measurements of total phosphorus (TP) and total reactive phosphorus (TRP) with a molybdenum blue method (Phosphax, Hach Lange) and turbidity, nitrate-nitrogen (NO_3-N), dissolved organic carbon with optical sensors (Spectrolyser, Hach Lange) at the outlet. Along the stream network turbidity and specific conductivity are measured with optical sensors (EXO2, YSI). Long-term water quality monitoring for TP, soluble reactive phosphorus (SRP), particulate phosphorus (PP), NO_3-N and suspended sediments (SS) has been carried out since 1988, using both grab and flow-proportional sampling at the outlet and along the stream network (Kyllmar et al., 2014). Tullstorp is monitored at three different gauge locations for water stage and water quality (Hallberg et al., 2024a; Wynants et al., 2024). Stream discharge in Tullstorp is estimated using established stage-discharge rating curves associated with continuous water stage data from pressure sensors (Hallberg et al., 2024a). Water quality measurements include continuous flow-proportional measurements of TP, SRP, PP, NO_3-N and SS at downstream locations and continuous measurements of turbidity, dissolved oxygen, specific conductivity and fluorescent organic matter with optical sensors (EXO2, YSI) at the upstream and midstream locations, supplemented with regular manual grab sampling.

2.2. Hydrochemical model

The catchment models were set-up in Hydrological Predictions of the Environment (HYPE), which is a semi-distributed and open source hydrological and nutrient transport modelling framework. HYPE has been designed for Swedish and European environments and has demonstrated good ability to model water quantity and quality dynamics (Lindström et al., 2010). Moreover, HYPE has routines that allow modelling desired reduction in nutrients and sediments under future climate scenarios (Bartosova et al., 2019; Capell et al., 2021). The catchment models building blocks consist of combinations of soil type and land use classes (SLCs), with 27 SLCs in Hestad, and 60 SLCs in Tullstorp. For each SLC, the soil system was classified with up to three soil layers with defined depths, tile drain depths, and different soil chemistry and physical characteristics. Crop types were specified together with the ploughing dates and application of mineral fertiliser and manure, based on data from nearby agricultural monitoring catchments (Kyllmar et al., 2014). Besides fertilisation, nutrients enter the modelled catchment through atmospheric deposition and rural sewage, and leave through crop uptake, denitrification, and with stream water discharge (Lindström et al., 2010). Potential crop nutrient uptake is based on a logistic growth equation throughout the growing season. The actual nutrient uptake of crops is limited by the available nutrients and a temperature function. Starting pools of nutrients in the different soil layers, as active compounds, in organic form, and bound to soil particles were specified for different SLCs. The values were based on regional trends from the Swedish national soil databases comprising thousands of soil samples (Strömqvist et al., 2012). Rainfall is assumed to fall uniformly across the catchment and is split into different fractions depending on soil and vegetation physical characteristics: surface runoff, soil infiltration, subsurface runoff (phreatic groundwater), and tile drainage. Groundwater depth responds to the amount of infiltration, evapotranspiration, and runoff, while tile drainage becomes activated when the groundwater level raises above the tile drain depth. Nutrient and sediment runoff amounts are governed by the runoff intensity, runoff pathways, and the soil chemistry in the different SLC soil layers.

The models were forced with daily average precipitation and temperature data. Empirical daily nutrient loads were derived from flow-proportional nutrient concentrations using daily discharge values. The model was optimised using the combined manual and automatic calibration based on the Differential Evolution Markov Chain (DE-MC) algorithm (Braak, 2006). The calibration was carried out following a stepwise approach by identifying key parameter groups and calibrating these together within possible ranges, while keeping other parameters fixed to reduce potential equifinality (Strömqvist et al., 2012). Since nutrient and sediment transport is largely governed by hydrology, the model was first calibrated for discharge. Water quality was calibrated using nutrient and sediment loads from flow-proportional sampling, which reduces uncertainty in concentration measurements during low and high flows (Kyllmar et al., 2014). A smaller subsample of the entire dataset was used to temporally validate the model setups for uncalibrated periods, prioritising the available data for calibration to yield more robust models (Shen et al., 2022). The simulation results were evaluated by comparing daily discharge, and nutrient and sediment loads with observations, using a set of goodness-of-fit indicators (Moriasi et al., 2015). The fits of simulated results varied from satisfactory to very good. Further details on the set-up procedures, model assumptions, calibration and validation can be found in (Wynants et al., 2024).

2.3. Future climatic scenarios

We used an ensemble of three general circulation models (GCM) from the Coupled Model Intercomparison Project Phase 5 (CMIP5). The models were the "Met Office Hadley Centre ESM, HadGEM2-ES" (Jones et al., 2011), the "Max Planck Institute ESM-LR" (Popke et al., 2013), and the "ICHEC-EC-EARTH" (Hazeleger et al., 2010). These GCMs simulate representative concentration pathways (RCPs) 2.6 (stringent reduction), 4.5 (moderate), and 8.5 (business as usual) (Collins et al., 2013). The GCMs were downscaled to a 5 km grid over the northern European regions using the "KNMI regional atmospheric climate model (RACMO) version 2" (van Meijgaard et al., 2008) and the "SMHI Rossby Centre regional climate model" (SMHI-RCA4) (Strandberg et al., 2015). An overview of the downscaled climate models can be found in Table S1 and (Wynants et al., 2024). Outcomes from these downscaled climate models were statistically scaled against a reference temperature and precipitation dataset using the distribution-based scaling algorithms of Yang et al. (2010). The resulting daily temperature and precipitation data were used to drive the HYPE model for predicting changes in nutrient and sediment concentrations and loads under future climatic conditions. Agricultural management and the growing season length were assumed to remain the same under different climate trajectories.

2.4. Data analyses

All data analyses were performed in Matlab version 9.13.0 (R2022b) with the Statistics toolbox version 9.4 (R2022b) (The MathWorks Inc., 2022) and R version 4.2.1 (R Core Team, 2022). The Fathom toolbox (Jones, 2017) was used for redundancy analysis and package *hydrostats* (Bond, 2022) for analysis of hydrological data including estimation of the baseflow index.

We used model predictions to evaluate the differences in flow metrics, concentrations and loads between baseline (1995–2023) and future climatic conditions (2024–2099). We conducted comparisons between both periods based on modelled flow and water quality data. This allowed for direct comparisons and minimised overrepresentation of extreme concentrations and loads captured with high-frequency data in baseline conditions. The measured data including high-frequency flow and water quality was used solely to calibrate and validate the model outcomes. Flow predictions during baseline conditions were based on measured precipitation data. For future conditions, flow was simulated based on different climatic models. Flow metrics included median flow (Q_{med}), flashiness index (Q_5/Q_{95}), coefficient of variation (CV), baseflow index (BFI) and stream drought index (SDI). The flashiness index was calculated as the ratio of top 5th percentile flows to lowest 95th percentile flows (Ulén et al., 2016). The SDI was calculated as in (Nalbantis and Tsakiris, 2008), with SDI > 0 indicating normal wetness conditions and mild drought for values $-1 <$ SDI < 0.

For all data inputs and model outputs we used a Shapiro-Wilk test in R to test the normality of data. As the data differed in distribution, we used both parametric (*t*-tests) and non-parametric (Kruskal-Wallis) tests to compare the model predictions with empirical measurements during the baseline period. These methods also helped evaluate differences between the climate models and RCPs, as well as test the significance of projected changes in flow, concentrations and loads. Percentage change between metrics for baseline and future conditions was calculated. When comparing baseline and future conditions, we used unweighted ensembles of climatic models for the respective RCPs calculated as median values of the three climatic models (ICHEC, KNMI, MPI). We did not weigh the ensemble models because no single climate model was shown to perform better under baseline conditions (Wynants et al., 2024), and this approach allowed us to quantify uncertainty (Haughton et al., 2015; Tebaldi and Knutti, 2007). Herein, variation in flow and chemical metrics was assessed against prediction errors resulting from different climatic models by calculating the relative median absolute deviation (RMD) as the median absolute deviation divided by median and expressed in percentage.

To characterise solutes' (NO_3-N and SRP) and particulates' (PP and SS) behaviour in relation to changing flow conditions, linear slopes of the C-Q relationships were calculated on concurrent log10-transformed data. Near-zero slopes ($-0.1 <$ slope < 0.1) indicate a chemostatic C-Q pattern, positive slopes indicate a chemodynamic concentration response and negative slopes indicate a chemodynamic dilution response (Bieroza et al., 2018). We used high-frequency water quality data from both catchments to check if the modelled C-Q slopes during baseline conditions were realistic. To elucidate sources of solutes and particulates in the study catchments, we apportioned flow into three hydrological pathways modelled by HYPE: tile runoff, surface runoff and groundwater runoff. For each flow pathway, C-Q slopes were calculated separately both for baseline and future conditions. As near zero slopes cannot give evidence for small variation in concentration variability and can potentially lead to false interpretations of solute/sediment flow dependencies (Musolff et al., 2015), we used a complementary approach. We calculated the ratio of RMD for concentrations and flow (RMD_{conc}/RMD_Q) consistently with previously tested CV_{conc}/CV_Q in the literature (Thompson et al., 2011). The interpretation of the RMD_{conc}/RMD_Q and CV_{conc}/CV_Q against the C-Q slope is similar, with $RMD_{conc}/RMD_Q < <1$ $CV_{conc}/CV_Q < <1$ and slope $< <1$ indicating a chemostatic C-Q pattern.

To evaluate the impact of future climate on solute and particulate mobilisation and transport, we calculated mobilisation and delivery indices (Mellander et al., 2022). The mobilisation index is defined as the ratio of highest to lowest concentrations and the delivery index as the ratio of highest to lowest loads normalised to median, similar to Q_5/Q_{95}. Daily concentrations were aggregated to seasonal values of indices and to entire hydrological years (October – September). Spearman pairwise linear correlation and redundancy analysis were performed to evaluate the relationships between mobilisation and delivery indices and explanatory variables. Explanatory variables included season (Season), mean air temperature (Temp), total precipitation (Prec), total evaporation (Evap), flow volume (Q_{vol}), Q_{med}, Q_5/Q_{95}, SDI, median concentration (Conc), total load (Load), and variables directly derived from the HYPE model: groundwater depth (Gw), dominant flow pathway (Flowpath), denitrification rate (Den), nutrient crop uptake (Crop), mineralisation rate (Min), soil P pool (P pool). Categorical variables, Season and Flowpath were represented by numeric indices: autumn 1, winter 2, spring 3, summer 4 and tile 1, surface 2 and groundwater runoff 3 respectively. Hydrological seasons were defined as follows: autumn October–December, winter January–March, spring April–June and summer July–September. Due to differences in catchment storage and the length of flow pathways between the catchments, there might be a delay in response of mobilisation/delivery indices to explanatory drivers. Therefore, we have also calculated Spearman correlations with a time lag of 6 months indicating that current values of indices were correlated against the values of explanatory variables delayed by 6 months. The time lag value of 6 months was chosen based on the cross-correlation analysis between the indices and explanatory variables.

3. Results

3.1. Hydrological response

The differences in catchments' size and dominant soil texture are reflected in flow metrics during baseline hydrologic conditions (1995–2023; Table 1). The larger and loam-dominated Tullstorp catchment has median flow an order of magnitude larger than the smaller and clay loam-dominated Hestad catchment. Both catchments exhibit significant flashiness in hydrologic response, measured with Q_5/Q_{95}, particularly during autumn. The Tullstorp catchment despite higher BFI of 0.41, indicating a significant input of groundwater, is also flashier than tile drainage dominated Hestad catchment. The catchments are generally not at risk of stream drought (measured with SDI). On a seasonal basis, both catchments show a similar hydrological regime with low flows during summers and highest flows during winters.

Climate change will lead to increases in the mean air temperature by 18 % (median value of the three climatic models) in both catchments with largest increases during autumn by 39 % in Hestad and 22 % in Tullstorp (Table 1). Precipitation is forecasted to increase by 18 % in Hestad and 3 % in Tullstorp. However, large seasonal differences are also expected. Hestad will have a slight increase during autumn and winter in Hestad, whilst Tullstorp will experience a large decrease 31 % in winter precipitation. Both spring and summer precipitation is predicted to significantly increase in both catchments, e.g., spring precipitation in Hestad will increase 54 %. Increased precipitation will lead to flows 80 % higher in Hestad and 16 % in Tullstorp, with similar flow patterns in all combinations of climatic scenarios and models (Table 1 and Fig. 1). However, the increases in flow will not be uniform between the catchments. In Hestad, the greatest increase in median flow will occur during spring and summer (104 and 125 % respectively). In Tullstorp the largest increases in flows will be shifted towards summer and autumn (93 and 155 % respectively). In Tullstorp, a significant 95 % decrease in spring flows will occur, most likely due to significantly reduced winter precipitation and increased spring temperatures. The changes in flow patterns will be accompanied by changes in flashiness. Flashiness will decrease during winter and increase during summer in

Table 1
Annual and seasonal variation in hydroclimatic metrics for baseline (1995–2023) and future (2024–2099) climatic conditions for three emission scenarios: low RCP2.6, medium RCP4.5 and high RCP8.5.

	Temp (°C)		Prec (mm)		Q_{med} (m^3s^{-1})		RMD (%)		Q_5/Q_{95} (−)		BFI (−)		SDI (−)	
	H	T	H	T	H	T	H	T	H	T	H	T	H	T
Baseline annual	7.3	8.2	578	822	0.014	0.38	77.0	71.2	102	145	0.20	0.37	0.89	0.32
Autumn	3.5	5.8	175	234	0.021	0.08	89.1	98.2	226	2306	0.19	0.21	0.94	0.36
Winter	1.3	2.6	129	261	0.053	0.80	77.2	52.7	58	56	0.22	0.50	0.20	0.18
Spring	11.1	10.6	98	148	0.007	0.68	76.8	53.1	135	20	0.22	0.50	0.93	0.31
Summer	16.0	14.5	176	178	0.001	0.05	46.2	89.3	68	234	0.12	0.25	0.86	0.34
RCP2.6 annual	8.2	9.4	669	817	0.032	0.45	76.0	90.6	121	658	0.20	0.38	0.35	0.05
Autumn	4.4	6.6	164	235	0.042	0.65	91.4	92.2	208	2357	0.20	0.36	0.75	0.51
Winter	0.3	2.2	130	182	0.083	1.03	72.9	48.1	39	15	0.25	0.59	0.60	0.69
Spring	11.6	11.7	166	169	0.023	0.24	79.1	91.6	113	231	0.19	0.41	0.09	−0.41
Summer	16.5	17.2	209	230	0.006	0.14	61.8	89.6	130	1084	0.12	0.17	−0.66	−0.70
RCP4.5 annual	8.8	10.0	702	846	0.036	0.48	74.8	88.7	129	581	0.18	0.35	0.38	0.17
Autumn	4.9	7.0	183	251	0.052	0.71	93.0	86.4	219	1479	0.19	0.34	1.28	0.76
Winter	1.2	2.8	130	190	0.089	1.07	71.3	48.1	34	17	0.27	0.61	0.76	0.78
Spring	12.2	12.3	171	175	0.020	0.25	78.3	92.1	128	269	0.18	0.37	0.00	−0.43
Summer	17.1	17.8	218	230	0.008	0.14	62.7	90.9	129	893	0.11	0.17	−0.61	−0.68
RCP8.5 annual	9.9	10.9	712	868	0.032	0.42	75.7	90.7	144	683	0.19	0.34	0.47	0.00
Autumn	6.2	8.1	184	258	0.042	0.62	91.7	97.7	225	1861	0.18	0.32	0.98	0.55
Winter	2.1	3.8	139	200	0.088	0.98	71.5	49.3	38	16	0.26	0.58	0.91	0.63
Spring	12.9	13.0	178	182	0.022	0.21	79.8	91.6	131	292	0.19	0.36	0.02	−0.55
Summer	18.2	18.8	212	229	0.006	0.07	64.7	89.8	158	1075	0.11	0.13	−0.69	−0.64
Future median	8.7	9.8	695	846	0.032	0.45	75.3	90.7	129	672	0.19	0.35	0.39	0.06
Autumn	5.2	7.3	183	251	0.042	0.65	91.7	92.2	219	1861	0.19	0.34	0.98	0.55
Winter	1.2	2.9	130	190	0.088	1.03	71.5	48.1	38	16	0.26	0.59	0.76	0.69
Spring	12.3	12.4	171	175	0.022	0.24	79.1	91.6	128	269	0.19	0.37	0.02	−0.43
Summer	17.3	17.9	212	230	0.006	0.14	62.7	89.8	130	1075	0.11	0.17	−0.66	−0.68
% change	17.8	17.9	18.4	2.9	79.7	15.6	−2.2	24.1	23.6	129.0	−7.8	−4.6	−78	−136
Autumn	39.0	22.3	4.4	7.0	68.2	154.2	2.9	−6.2	−3.2	−21.4	−2.2	49.5	4	42
Winter	−7.6	11.7	0.8	−31.5	50.8	25.0	−7.7	−9.0	−41.1	−113.1	17.9	17.2	117	119
Spring	9.9	15.3	53.9	16.8	104.4	−94.5	3.0	53.2	−5.7	171.7	−13.5	−29.9	−190	1259
Summer	7.8	21.3	18.4	25.1	124.5	93.3	30.2	0.5	62.6	128.6	−9.3	−37.3	−1550	590

Notes: Future seasonal predictions were calculated as median values of the three climatic models (KNMI, ICHEC, MPI) per RCP. Annual values for Baseline and RCPs were calculated as median values of seasonal values apart from precipitation for which total value was taken. Future median is a median value of annual values for all RCPs. Percentage change was calculated as a difference between baseline and future annual values divided by their average and expressed in %. Study catchments: Hestad H and Tullstorp T. Metrics include mean air temperature (Temp), total precipitation (Prec), flow median (Q_{med}), flow relative median absolute deviation (RMD), flashiness index (Q_5/Q_{95}), baseflow index (BFI) and stream drought index (SDI).

Hestad and spring and summer in Tullstorp. Under future climate, reduced flashiness during winters will be driven by a lower contribution of the highest flows, within the top 20th percentile of flows (Fig. S2). During the periods of increased flashiness (summer in Hestad and spring and summer in Tullstorp), mild drought conditions (SDI between 0 and-1) will prevail in both catchments. Prediction errors due to differences in climatic models for all hydroclimatic parameters are generally much lower than forecasted seasonal changes under future climate (Table S2).

The changes in future flow conditions will be accompanied by a relative change in the distribution of dominant flow pathways (Table S3). Tile and groundwater runoff are the major flow pathways in Hestad during autumn/winter and spring/summer while in Tullstorp groundwater runoff dominates (81 %) all year round, which is also corroborated by the BFI results (Table 1). In the future conditions, tile runoff will dominate in Hestad. In Tullstorp, the importance of tile and surface runoff will increase except during spring when there will be a significant flow reduction.

3.2. Hydrochemical response

Although the catchments have different flow dynamics, concentrations of solutes and particulates in both are generally high and within similar range (Fig. 2 and Table S4). This suggests the presence of easily mobilised and abundant sources. The only marked difference between the catchments is in median NO_3-N concentrations, which were considerably lower in Hestad compared to Tullstorp (0.52 and 4.15 mgl^{-1} respectively). The highest concentrations of most parameters occurred during the highest winter flows. In Tullstorp, there is a clear seasonal pattern in concentrations increasing in autumn, reaching their maximum in winter, and then decreasing towards summer minimum. In Hestad, this pattern is visible only for NO_3-N. SRP concentrations in both catchments are highest in autumn and decrease towards the summer. Loads, as expected from difference in median flow, are an order of magnitude higher in Tullstorp and show a seasonal pattern consistent with the changes in flow (Fig. S3 and Table S7). The majority of the annual load is derived from the top 10 % of flows. In Hestad these occur mostly in winter. In Tullstorp they occur predominantly in spring, with summer loads being negligible. The top 10 % of flows contribute between 72 % of cumulative load for NO_3-N to 55 % for SRP in Hestad, while in Tullstorp this range varies from 60 % for PP to 45 % for SRP (Fig. S1).

Greater flashiness and large seasonal differences in flow conditions will lead to significant changes in future concentrations (Fig. 2 and Table S4) and loads (Fig. S4 and Table S7). There will also be marked differences between parameters, seasons and catchments. The largest annual change in concentrations will be seen in NO_3-N, which will increase by 34 % in Hestad and decrease by 62 % in Tullstorp. The differences between seasons will be even more pronounced. Concentrations of NO_3-N will decrease in winter (−29 % in Hestad and −17 % in Tullstorp). A large increase will occur during summer in Hestad (154 %) and autumn and summer in Tullstorp (152 and 118 %). Spring NO_3-N concentrations in Tullstorp will decrease by −168 % due to much reduced flows. Similarly, there will be larger differences in concentrations for SRP, PP and SS between the seasons than between the catchments. Greatest concentration increases will occur in summer for Hestad and autumn and summer for Tullstorp. Correspondingly, due to the lower streamflow, spring concentrations of SRP, PP and SS in Tullstorp will decrease by −156, −42 and −49 % respectively. These

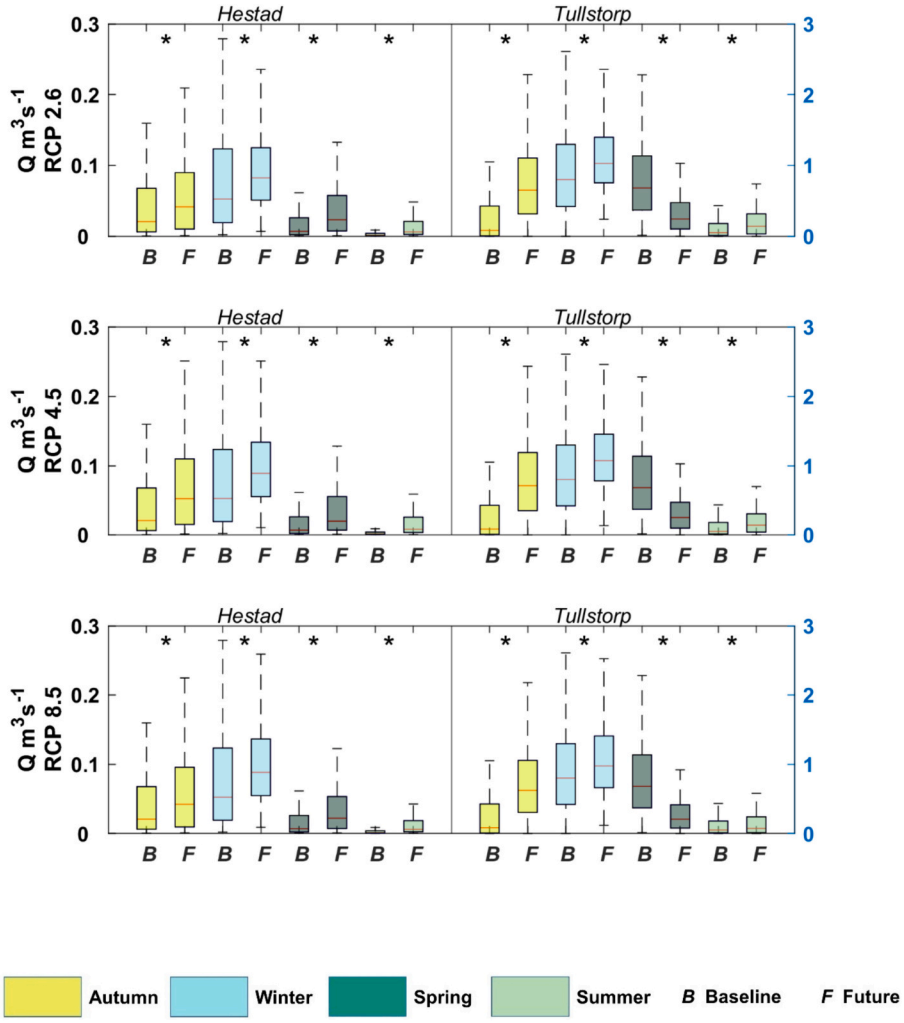

Fig. 1. Stream flow for baseline (*B*) and future (*F*) climatic conditions per season (indicated with different colors). The left-hand vertical axis is the flow for Hestad and the right-hand axis is the flow for Tullstorp. Future seasonal predictions were calculated as median values of the three climatic models (KNMI, ICHEC, MPI) per RCP. Statistically significant differences (Kruskal-Wallis test, at 0.05 significance level) are indicated with *. Boxplots: the central red line indicates the median, and the bottom and top edges of the box indicate the 25th and 75th percentiles, respectively. The whiskers extend to the most extreme data points not considered outliers; the individual outliers were not plotted.

forecasted changes in concentrations seem credible as variation in concentrations (Table S6) is consistent between baseline and future conditions and the prediction errors are generally much lower (Table S5).

Differences in loads between baseline and future conditions will be generally much larger than differences in concentrations, particularly for solutes. In Hestad, annual NO3-N loads will increase by 131 %, while SS will increase by 78 % and SRP by 60 %. In Tullstorp, NO3-N loads will decrease by 31 %, with SRP increasing by 101 % and SS by 23 %. On a seasonal basis, the variation in loads will be even larger, with the greatest increases (>100 %) during spring and summer in Hestad and summer and autumn in Tullstorp. Large decreases will occur in Tullstorp during spring (from −111 % for SS to −180 % for NO_3-N). Due to reduced winter flashiness, the contribution of the top 10 % of flows to annual loads will be lower compared to baseline conditions, from 30 % for SS to 35 % for NO_3-N in Hestad and from 25 % for SRP to 35 % for NO_3-N in Tullstorp (Fig. S2). Forecasted changes in loads are much larger than prediction errors (Table S8) and there is no shift in seasonal variations in loads between baseline and future scenarios (Table S9).

Concentration-discharge (C-Q) slopes indicate when solutes and particulates are mobilised and delivered to the stream in relation to flow conditions. Solutes and sediments in the study catchments show overall mostly positive, chemodynamic slopes. This indicates that concentrations increase proportionally to flow during spring and summer with a shift towards more chemostatic slopes in winter (Table S10). There are also differences in C-Q slopes between different flow pathways (Fig. S4a-d), with groundwater runoff showing much steeper positive slopes compared to both tile and surface runoff that tend to oscillate around chemostasis (near-zero slopes). NO_3-N and SS slopes are both consistent between the catchments and seasons, while SRP and PP show the largest variation. SRP slopes indicate dilution in both catchments during autumn, weak positive chemodynamic and chemostatic slopes during winter and summer and strong positive chemodynamic response during spring. For PP, Hestad exhibits dilution during all seasons apart from weak chemostasis in winter, while in Tullstorp chemodynamic slopes dominate all year round with near chemostatic slopes during summer. In the future, the concentration-discharge relationships will largely remain the same for NO_3-N and SS with a general tendency for lower slopes and RMD_{conc}/RMD_Q for SRP and PP (Table S10).

3.3. Mobilisation and delivery patterns and their drivers

The mobilisation index, which is the range between highest and lowest concentrations, is generally higher and more variable in Tullstorp

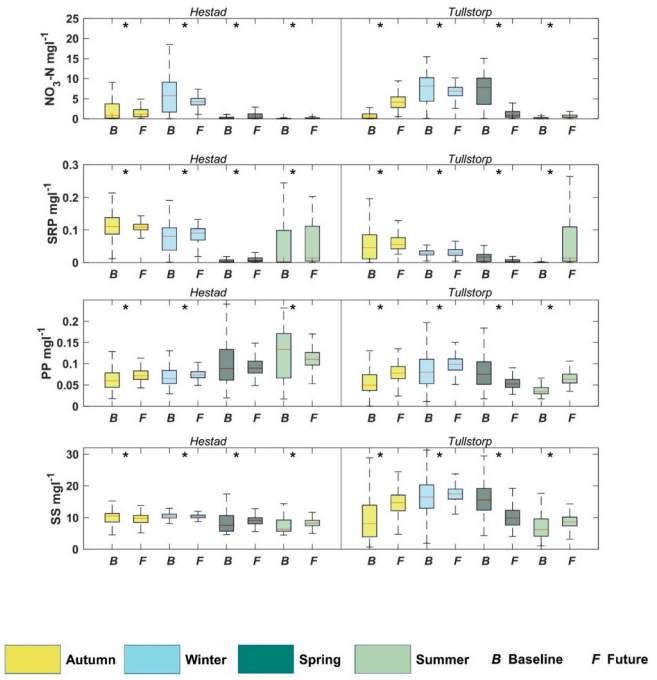

Fig. 2. Stream concentrations for baseline (*B*) and future (*F*) climatic conditions per season (indicated with different colors). Nitrate-nitrogen (NO_3-N), soluble reactive phosphorus (SRP), particulate phosphorus (PP), suspended sediments (SS). Boxplot description as in Fig. 1.

except for NO3-N in Hestad (Fig. 3 and Table S11). The highest mobilisation index values are observed for solutes while particulates have much lower values, e.g. for NO_3-N 18.1 and 7.7 and for SS 1.9 and 2.1 in Hestad and Tullstorp respectively. On a seasonal basis, the mobilisation index is the greatest during spring and summer, and with much lower values during winter. Summer and spring values also show large variation (Table S13). The future mobilisation index will generally be higher compared to baseline conditions. This is particularly true for solutes, with forecasted changes being larger than the prediction error (Table S12).

The delivery index, which is the range between highest and lowest loads, follows similar pattern as the mobilisation index (Fig. 4 and Table S14), with higher delivery indices for Hestad, solutes, and summers. There is also a much larger variation in delivery index for each parameter and season (Table S16) compared to the mobilisation index. High values of delivery index occur during summer, with the highest values reaching 1000 for NO_3-N and 200 for SRP and SS. In Tullstorp the corresponding values do not exceed 50 for NO_3-N, 200 for SRP and 100 for SS. The model predicts significant increases in the delivery index under future climate, particularly during spring and autumn for NO_3-N and spring and summer for SRP, PP and SS. On average, the delivery index will increase from 112 % for SRP, 111 % for NO_3-N to 28 % for PP in Hestad and from 50 % for SRP to 28 % for PP in Tullstorp (Table S14) and are larger than the prediction errors (Table S15).

The mobilisation and delivery indices are highly correlated, with Spearman's correlation coefficient ranging from 0.49 for SRP to 0.65 for NO_3-N in Hestad and from 0.45 for NO_3-N to 0.66 for SS in Tullstorp (Table S17). For the mobilisation index, the best predictors for the future climatic conditions vary between parameters. There are many strong correlations between environmental variables and NO_3-N mobilisation index, particularly for Hestad (positive Temp 0.63, Evap 0.53, Min 0.57, Season 0.54 (increase towards summer) and negative SDI -0.51 and Gw −0.64). For Tullstorp, the correlations with the concurrent values of environmental variables are generally weaker than for time-lagged values (−6 months), indicating a delay in mobilisation response, with positive correlations for Gw 0.55 and negative for Temp −0.65, Evap −0.62 and Season −0.77. For SRP, the strongest correlations are for current and past values of Temp, Evap and Gw with Season being only

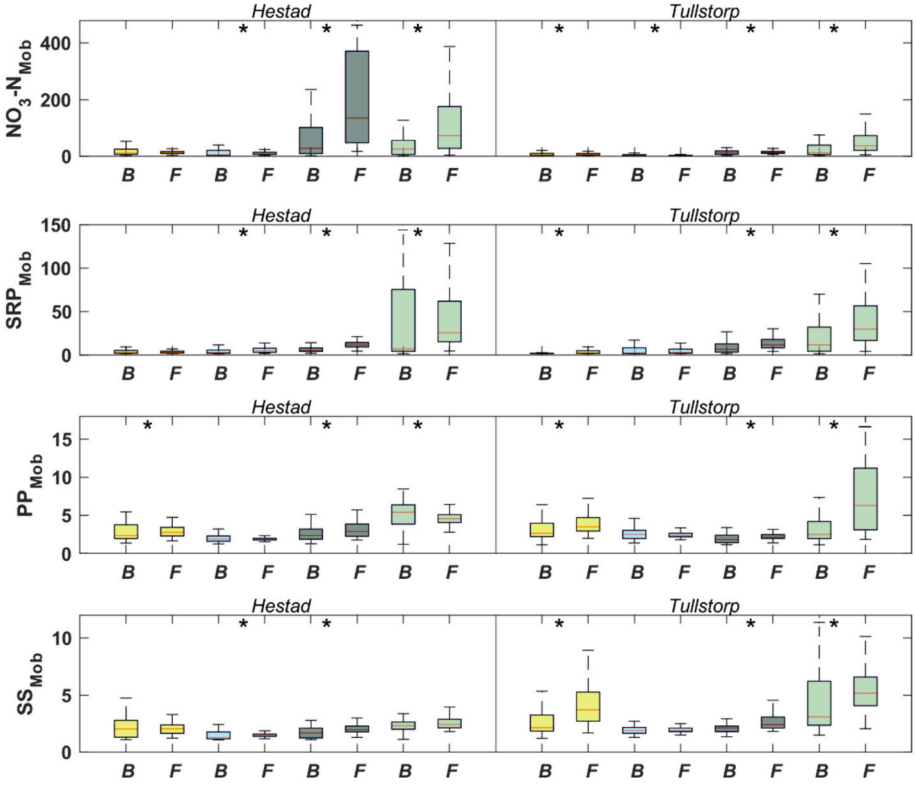

Fig. 3. The mobilisation index for baseline (*B*) and future (*F*) climatic conditions per season (indicated with different colors). Nitrate-nitrogen (NO_3-N), soluble reactive phosphorus (SRP), particulate phosphorus (PP), suspended sediments (SS). Boxplot description as in Fig. 1.

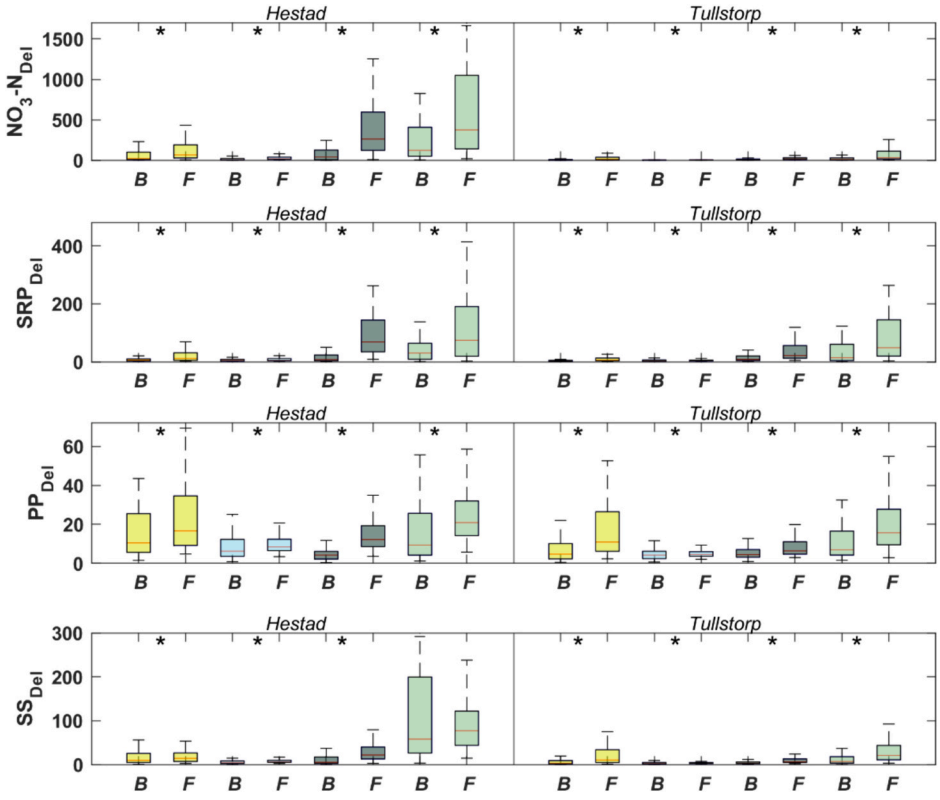

Fig. 4. The delivery index for baseline (*B*) and future (*F*) climatic conditions per season (indicated with different colors). Nitrate-nitrogen (NO_3-N), soluble reactive phosphorus (SRP), particulate phosphorus (PP), suspended sediments (SS). Boxplot description as in Fig. 1.

significant predictor for Tullstorp (0.79). There were generally fewer strong correlations for PP and SS, with Season being a predictor in both catchments and Q_5/Q_{95} being a strong predictor in Hestad. In Tullstorp, SS mobilisation is driven by lagged Temp, Evap and Gw conditions. Correlations for the delivery index were generally weaker. Larger differences occur between the catchments (Table S18), although they largely mimic the patterns shown by the mobilisation index. For solutes, Temp, Evap, Gw and Season are the most important predictors with concurrent and time-lagged values in Hestad and Tullstorp for SRP but only time-lagged for NO_3-N in Tullstorp. Season is also the best predictor

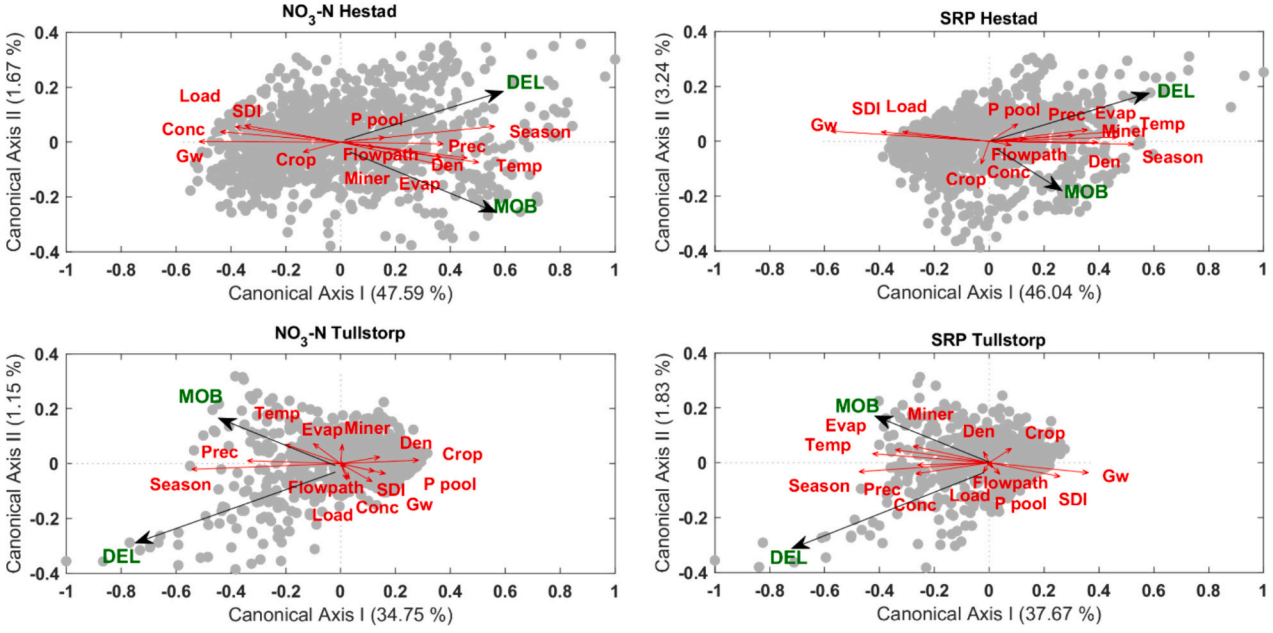

Fig. 5. Redundancy analysis for NO_3-N and SRP in Hestad (top panel) and Tullstorp (bottom panel) catchments. Response variable: mobilisation and delivery indices, explanatory variables: mean air temperature (Temp), total precipitation (Prec), total evapotranspiration (Evap), stream drought index (SDI), mean concentration (Conc), groundwater depth (Gw), total load (Load), dominant flow pathway (Flowpath), denitrification rate (Den), nutrient crop uptake (Crop), mineralisation rate (Min), soil P pool (P pool), and season (Season). Variance explained by each canonical axis is given in brackets.

of delivery index for PP and SS. However, these environmental variables interact to influence the mobility and delivery responses, as demonstrated in the multivariate redundancy analysis (Fig. 5). Overall, it seems that NO_3-N and SRP mobility in both catchments is positively driven by weather conditions (temperature, evapotranspiration, precipitation, and season) and negatively associated with groundwater depth, mean load and concentration, stream drought index, crop uptake. Solute delivery is also positively associated with weather factors, mostly season, and negatively associated with groundwater depth, stream drought index, denitrification, and crop uptake.

4. Discussion

4.1. Effects of climate change on hydrological response

Climate change generally leads to more varied and flashy stream hydrographs and steeper flow distributions, driven by larger seasonal differences between the highest and lowest flows, in temperate catchments (Grusson et al., 2021; Li et al., 2024; Payne et al., 2020). Contrary to this, under future climate predictions, we observed a more even distribution of flows throughout a hydrological year with higher lowest flows and lower highest flows respectively (Fig. 1 and S2). This could be partly attributed to the general underprediction of rainfall variance and extreme events in future climate models (Fig. S5). The use of an ensemble climate forecast approach provided an uncertainty range of the forecasted nutrient loads. However, climate models still struggle to accurately predict extreme precipitation events (Krysanova et al., 2020; La Follette et al., 2021; Shamekh et al., 2023). Uncertainties are expected to decrease with improved climate forecasting under CMIP6 (Jacob et al., 2020; Krysanova et al., 2018), however these improved models were not yet available for our study catchments. Since the baseline models in our study were driven by empirical rainfall measurements, the variance in the future flow scenarios was likely underestimated, leading to observed flow averaging. Despite more uniform hydrographs in general, both study catchments will experience large seasonal differences in precipitation and flow conditions in the future, with significant and consistent increases in summer flows (Fig. 1). In Tullstorp, shifts in hydrological response are expected due to the predominance of groundwater flow pathways, which generally respond more slowly compared to the flashier response seen in Hestad. For example, the spring/summer flow increases in Hestad will occur during summer/autumn in Tullstorp. What is striking about the forecasted future flows, is the large magnitude of change e.g., summer flows will increase >100 % in both catchments with large differences between seasons e.g., a −95 % decrease in flows during spring followed by a 93 % increase in summer flows in Tullstorp (Table 1). This will lead to both wetter and drier conditions compared to the baseline scenario and more rapid transitions between the hydrologic extremes. For example, an overall increase in summer flows will be accompanied by a higher risk of stream drought. The acceleration of the water cycle observed in our study catchments will be most likely driven by a greater importance of the superficial and flashy flow pathways of tile and surface runoff (Table S2). Surprisingly, this pattern will be consistent in both catchments despite marked differences in the overall flow pathway distribution, i.e., tile-runoff dominated Hestad and groundwater-dominated Tullstorp. This suggests that agricultural catchments will in general become flashier under climate change, with a higher risk for both extreme floods and droughts. Other studies indicated similar patterns in agricultural catchments, with increased total precipitation and frequency of high-intensity precipitation events but constant or even reduced soil water content (Grusson et al., 2021). This can be explained by increased air temperature and evapotranspiration leading to reduced soil moisture and groundwater recharge that in turn will activate more superficial flow pathways during precipitation events. Another consequence of forecasted increase in air temperature will be reduced importance of snowmelt events and shorter freeze-thaw cycles (Liu et al., 2019). This is particularly relevant in Hestad catchment with its more continental climate, potentially contributing to more homogenised flow distributions throughout the hydrological year.

4.2. Effects of climate change on hydrochemical response

The effects of extreme hydrological events, droughts and floods, on solute and sediment mobilisation and delivery depend primarily on the apportionment of their pools between different catchment compartments and flow pathways (Stewart et al., 2022). We found that hydrograph homogenisation (Fig. S2) will lead to more even distribution of solute and sediment concentrations and loads over the seasons (Fig. 2 and S3). We linked this pattern with significant increases in mobilisation and delivery of solutes and sediments during the warmer part of the year (Figs. 3–4). This is a surprising finding compared to previous studies indicating high importance of increased winter flashiness (Ockenden et al., 2017). The observed shift in mobilisation and delivery regimes was consistent for both catchments. This could be a general pattern for agricultural catchments in Northern Europe driven by combined changes in air temperature and precipitation. Using pairwise correlations between mobilisation indices and model parameters reflecting rates of dominant processes (Tables S17–18), we were able to show that higher nutrient mobilisation is driven by higher air temperatures leading to increased mineralisation of soil nutrients. At the same time, lower precipitation under climate change scenarios reduces the groundwater depth and extends the oxic conditions in soils which further reinforce mineralisation and accumulation of soil nutrients. Higher winter and spring temperatures can also increase the frequency of freeze-thaw cycles, contributing to higher nutrient mobilisation and delivery during spring (Klöffel et al., 2024). The more frequent activation of rapid and flashy pathways for tile and surface runoff will consequently mobilise and transport the accumulated soil nutrients and sediments to streams as a result. A combination of higher mobilisation and delivery of solutes and sediments during summer together with increased risk for stream drought will lead to major deterioration in water quality. Similar drivers of higher mobilisation and delivery were observed in both catchments (with a delayed response in Tullstorp) despite large differences in soil, land management and hydrological properties. This could be an indicator of limited resilience of catchments to hydrologic extremes and their transitioning to alternative stable states (Peterson et al., 2021). Therefore, the effects of accelerated hydrological and biogeochemical cycles driven by climate change can be general for highly modified and managed agricultural landscapes. This makes them critical ecosystems for mitigating the negative effects of climate change (Bieroza et al., 2024).

The clear changes in mobilisation and delivery patterns in both catchments were not reflected in the changes in C-Q relationships (Table S10 and Fig. S4). Only minor variation in C-Q slopes and the ratio RMD_{conc}/RMD_Q, with a weak tendency for more chemostatic responses under future climatic conditions were observed. Chemostatic slopes are linked with the presence of large and easily mobilised solute stores such as legacy sources in agricultural catchments (Bieroza et al., 2018; Rose et al., 2018). The observed minor shift towards chemostatic slopes could reflect a hydrograph smoothing and homogenisation of solute/sediment mobilisation and delivery across low and high flows. However, this also potentially suggests that legacy sources will continue to compound water quality impacts in the future, without major changes in agricultural practices (e.g., fertilisation) (Ockenden et al., 2017). Alternatively, the modelling approach that we adopted in this study might not properly reflect hydrological extremes and solute and sediment storage and exhaustion processes due to the lack of explicit model routines for legacy sources. This might suggest that the uncertainties of the climate forecasts were potentially amplified by uncertainties of the used hydrochemical model. We calibrated the hydrochemical model for current weather conditions, and it remains uncertain how representative the current model calibration will be for future climatic conditions.

Particularly non-linear responses to extreme weather, such as thresholds and hysteresis effects, are hard to predict under future climates (Krysanova et al., 2018; La Follette et al., 2021). HYPE is not a crop model and therefore does not account for the complex interactions with other environmental variables during crop growth and extended growing season resulting from climate change. Thus, accurately predicting the effects of climate change on solute/sediment mobilisation and delivery, along with their C-Q relationships, will likely require combining process-based hydrochemical models with kinetic biogeochemical models of legacy sources (Basu et al., 2022; Van Meter et al., 2017) and crop growth. Further, existing conceptualisation frameworks for interpreting C-Q relationships might be too simplified e.g., the effect of legacy sources on C-Q slopes (Bieroza et al., 2018; Godsey et al., 2019), highlighting the need for improved mechanistic understanding of their controls in diverse catchments and across spatial and temporal scales.

4.3. Implications for water quality and stream ecology, management, and remediation

Our work demonstrates the high value of integrating empirical and modelling approaches for making realistic predictions of future changes in mobilisation and delivery patterns controlling steam water quality. Significantly higher concentrations and loads driven by climate change will pose a challenge for water quality management in affected agricultural catchments. These challenges will likely extend to all downstream aquatic ecosystems. Large increases in summer concentrations together with increased temperatures will significantly increase the risk and frequency of detrimental algal blooms and hypoxia events (Diamond et al., 2023). Combined with flashier hydrological response and risk of drought, these stressors will also lead to overall increased pressures on stream biota (Birk et al., 2020; Woodward et al., 2016). These negative effects of climate change will require appropriate adaptation and mitigation measures beyond existing best management practices (BMPs) and remediation interventions. To effectively offset the increased solute and sediment mobilisation caused by changing climate, strategic planning is required. This planning must address the flashier delivery to streams and encompass all stages of the pollution continuum (Bieroza et al., 2020; Forber et al., 2018). A combination of catchment-based BMPs will be essential. These should include source and soil management strategies such as optimising fertilisation to crop requirements, reduced soil tillage. These practices could reduce accumulation and mobilisation of nutrients and sediments from agricultural soils (Withers et al., 2014). Additionally, edge-of field and in-stream measures to reduce pollution delivery to aquatic recipients will be necessary (Bieroza et al., 2024). Edge-of field measures such as constructed wetlands and integrated buffer zones prove particularly effective in reducing transport of diffuse agricultural pollution at critical delivery pathways like tramlines, gullies and tile drains (Carstensen et al., 2020; Djodjic et al., 2022; Hamback et al., 2023). In-stream remediation measures aiming at prolonging water residence times, regulating extreme flows and enhancing biogeochemical processing of solutes and sediments will be needed to reduce pollution transported along subsurface flow pathways (Hallberg et al., 2022; Riml et al., 2024). They have also potential to improve overall physicochemical conditions for stream biota (Birk et al., 2020; Stutter et al., 2018). In-stream measures are traditionally designed with a specific target, e.g., improving stream geomorphology and habitat diversity or reducing erosion and solute transport, and we urge for more multi-functional consideration of their effects. This would help the achievement of multiple environmental goals in a quicker and more cost-effective way (Bieroza et al., 2021). It would avoid undesired effects such as pollution swapping between diffuse pollution and greenhouse gas emissions (Hallberg et al., 2024b). We acknowledge that there is an important role of policy makers and funding schemes e.g., Common Agricultural Programme in European Union, to incentivise multi-functional adaptation and mitigation solutions, i.e. BMPs, edge-of field and in-stream measures, beyond particular interests or preferences of the involved stakeholders. Finally, in our study we only focused on hydrological and biogeochemical effects of climate change on water quality and did not consider other compounding factors such as socio-economic drivers, land use and land management change. Thus, any decisions and measures for climate change adaptation and mitigation should consider these additional drivers. Our modelling approach, which linked climate change scenarios with hydrology and biogeochemistry, could be supplemented with consideration of the Shared Socioeconomic Pathways (SSPs). This should particularly consider changing cropping regimes and fertiliser applications, providing more realistic and robust predictions of future water quality trajectories (van Vliet et al., 2023).

5. Conclusions

Climate change will lead to multiple negative effects on the structure and function of diverse ecosystems. These changes are already becoming clear in the ecosystems experiencing human disturbance, such us urbanisation or agricultural land use. These systems lack inherent buffering capacity to offset dramatic changes in hydrology and biogeochemistry. Our modelling results indicate a general acceleration of hydrological and biogeochemical responses in two agricultural catchments, leading to large seasonal differences in catchment wetness and runoff generation processes. Higher air temperature and evapotranspiration, coupled with more rapid freeze-thaw cycles and rainfall-runoff events, will increase the importance of flashy flow pathways. These pathways are responsible for rapid mobilisation and delivery of solutes and particulates to agricultural streams. The magnitude of predicted increases in solute and particulate mobilisation and delivery is much larger than the uncertainty associated with different climatic models. This suggests that the negative effects of climate change on water quality will be profound and significant. Deteriorating water quality together with the higher occurrence of extreme flood and drought events will pose a serious threat to stream biota and a considerable challenge to water management. It might be impossible to fully offset the climate change impacts in agricultural catchments solely with the best management practices, considering the prevalence and persistence of nutrient legacy sources. Thus, extensive efforts should be undertaken to mitigate the extent of global change impacts. To achieve the best cost-effectiveness and avoid potential pollution swapping effects, a systemic and landscape-oriented planning of mitigation should be prioritised over randomly placed and chosen individual measures. The effect of climate change on water quality in agricultural landscapes is complex and most likely non-linear. Therefore, there is a need for novel modelling frameworks considering both ecosystem and socio-economic responses, to reduce the uncertainty in the predictions and targeting of management and mitigation interventions.

CRediT authorship contribution statement

M.Z. Bieroza: Writing – original draft, Visualization, Validation, Supervision, Project administration, Methodology, Investigation, Funding acquisition, Formal analysis, Data curation, Conceptualization. **L. Hallberg:** Writing – original draft. **J. Livsey:** Writing – original draft. **M. Wynants:** Writing – original draft, Validation, Methodology, Formal analysis.

Declaration of competing interest

The authors declare that they have no known competing financial interests or personal relationships that could have appeared to influence the work reported in this paper.

Data availability

Data will be made available on request.

Acknowledgements

The funding for this research was supported by the Swedish Research Council Formas (grant 2018-00890), the Swedish Farmers' Foundation for Agricultural Research (grant O-21-23-537) and the Baltic-Waters2030 Foundation (grant B-2123), awarded to M. Bieroza. The authors would like to acknowledge Christoffer Bonthron and Johnny Carlsson from Tullstorpsån and Ståstorpsån remediation projects (https://tullstorpsan.se/) for their contributions.

Appendix A. Supplementary data

Supplementary data to this article can be found online at https://doi.org/10.1016/j.scitotenv.2024.175365.

References

Bartosova, A., Capell, R., Olesen, J.E., Jabloun, M., Refsgaard, J.C., Donnelly, C., et al., 2019. Future socioeconomic conditions may have a larger impact than climate change on nutrient loads to the Baltic Sea. Ambio 48, 1325–1336. https://doi.org/10.1007/s13280-019-01243-5.

Basu, N.B., Van Meter, K.J., Byrnes, D.K., Van Cappellen, P., Brouwer, R., Jacobsen, B.H., et al., 2022. Managing nitrogen legacies to accelerate water quality improvement. Nat Geo 15, 97–105. https://doi.org/10.1038/s41561-021-00889-9.

Bieroza, M.Z., Heathwaite, A.L., 2015. Seasonal variation in phosphorus concentration–discharge hysteresis inferred from high-frequency in situ monitoring. J. Hydrol. 524, 333–347. https://doi.org/10.1016/j.jhydrol.2015.02.036.

Bieroza, M.Z., Heathwaite, A.L., Bechmann, M., Kyllmar, K., Jordan, P., 2018. The concentration-discharge slope as a tool for water quality management. Sci. Total Environ. 630, 738–749. https://doi.org/10.1016/j.scitotenv.2018.02.256.

Bieroza, M., Bergstrom, L., Ulen, B., Djodjic, F., Tonderski, K., Heeb, A., et al., 2019. Hydrologic extremes and legacy sources can override efforts to mitigate nutrient and sediment losses at the catchment scale. J. Environ. Qual. 48, 1314–1324. https://doi.org/10.2134/jeq2019.02.0063.

Bieroza, M., Dupas, R., Glendell, M., McGrath, G., Mellander, P.-E., 2020. Hydrological and chemical controls on nutrient and contaminant loss to water in agricultural landscapes. Water 12, 3379. https://doi.org/10.3390/w12123379.

Bieroza, M.Z., Bol, R., Glendell, M., 2021. What is the deal with the Green Deal: will the new strategy help to improve European freshwater quality beyond the Water Framework Directive? Sci. Total Environ. 791, 148080 https://doi.org/10.1016/j.scitotenv.2021.148080.

Bieroza, M., Acharya, S., Benisch, J., ter Borg, R.N., Hallberg, L., Negri, C., et al., 2023. Advances in catchment science, hydrochemistry and aquatic ecology enabled by high-frequency water quality measurements. Environ. Sci. Technol. 1–32. https://doi.org/10.1021/acs.est.2c07798.

Bieroza, M., Hallberg, L., Livsey, J., Prischl, L.A., Wynants, M., 2024. Recognizing agricultural headwaters as critical ecosystems. Environ. Sci. Technol. 58, 4852–4858. https://doi.org/10.1021/acs.est.3c10165.

Birk, S., Chapman, D., Carvalho, L., Spears, B.M., Andersen, H.E., Argillier, C., et al., 2020. Impacts of multiple stressors on freshwater biota across spatial scales and ecosystems. Nat. Ecol. Evol. 4, 1060–1068. https://doi.org/10.1038/s41559-020-1216-4.

Blann, K.L., Anderson, J.L., Sands, G.R., Vondracek, B., 2009. Effects of agricultural drainage on aquatic ecosystems: a review. Crit. Rev. Environ. Sci. Technol. 39, 909–1001. https://doi.org/10.1080/10643380801977966.

Bol, R., Gruau, G., Mellander, P., Dupas, R., Bechmann, M., Skarbøvik, E., et al., 2018. Challenges of reducing phosphorus based water eutrophication in the agricultural landscapes of Northwest Europe. Front. Mar. Sci. 5, 1–16. https://doi.org/10.3389/fmars.2018.00276.

Bond, N., 2022. Hydrostats: Hydrologic Indices for Daily Time Series Data. CRAN.

Braak, C.J.F.T., 2006. A Markov Chain Monte Carlo version of the genetic algorithm Differential Evolution: easy Bayesian computing for real parameter spaces. Stat. Comput. 16, 239–249. https://doi.org/10.1007/s11222-006-8769-1.

Capell, R., Bartosova, A., Tonderski, K., Arheimer, B., Pedersen, S.M., Zilans, A., 2021. From local measures to regional impacts: modelling changes in nutrient loads to the Baltic Sea. Journal of hydrology. Reg. Stud. 36 https://doi.org/10.1016/j.ejrh.2021.100867.

Carstensen, M.V., Hashemi, F., Hoffmann, C.C., Zak, D., Audet, J., Kronvang, B., 2020. Efficiency of mitigation measures targeting nutrient losses from agricultural drainage systems: a review. Ambio 49, 1820–1837. https://doi.org/10.1007/s13280-020-01345-5.

Collins, M., Knutti, R., Arblaster, J., Dufresne, J.-L., Fichefet, T., Friedlingstein, P., et al., 2013. Long-term climate change: projections, commitments and irreversibility. In: Climate Change 2013: The Physical Science Basis. IPCC Working Group I Contribution to AR5. Cambridge University Press, Cambridge, UK and New York, USA, pp. 1029–1136.

Diamond, J.S., Moatar, F., Recoura-Massaquant, R., Chaumot, A., Zarnetske, J., Valette, L., et al., 2023. Hypoxia is common in temperate headwaters and driven by hydrological extremes. Ecol. Indic. 147 https://doi.org/10.1016/j.ecolind.2023.109987.

Djodjic, F., Geranmayeh, P., Collentine, D., Markensten, H., Futter, M., 2022. Cost effectiveness of nutrient retention in constructed wetlands at a landscape level. J. Environ. Manag. 324, 116325 https://doi.org/10.1016/j.jenvman.2022.116325.

Forber, K.J., Withers, P.J.A., Ockenden, M.C., Haygarth, P.M., 2018. The phosphorus transfer continuum: a framework for exploring effects of climate change. Agricultural & Environmental Letters 3. https://doi.org/10.2134/ael2018.06.0036.

Godsey, S.E., Hartmann, J., Kirchner, J.W., 2019. Catchment chemostasis revisited: water quality responds differently to variations in weather and climate. Hydrol. Process. 33, 3056–3069. https://doi.org/10.1002/hyp.13554.

Gómez, R., Arce, M.I., Sánchez, J.J., del Mar, Sánchez-Montoya M., 2011. The effects of drying on sediment nitrogen content in a Mediterranean intermittent stream: a microcosms study. Hydrobiologia 679, 43–59. https://doi.org/10.1007/s10750-011-0854-6.

Grusson, Y., Wesström, I., Svedberg, E., Joel, A., 2021. Influence of climate change on water partitioning in agricultural watersheds: examples from Sweden. Agric. Water Manag. 249 https://doi.org/10.1016/j.agwat.2021.106766.

Hallberg, L., Hallin, S., Bieroza, M., 2022. Catchment controls of denitrification and nitrous oxide emissions in headwater remediated agricultural streams. Sci. Total Environ. 836, 156513.

Hallberg, L., Djodjic, F., Bieroza, M., 2024a. Phosphorus supply and floodplain design govern phosphorus reduction capacity in remediated agricultural streams. Hydrol. Earth Syst. Sci. 28, 341–355. https://doi.org/10.5194/hess-28-341-2024.

Hallberg, L., Hallin, S., Djodjic, F., Bieroza, M., 2024b. Trade-offs between nitrogen and phosphorus removal with floodplain remediation in agricultural streams. Water Res. 258, 121770 https://doi.org/10.1016/j.watres.2024.121770.

Hamback, P.A., Dawson, L., Geranmayeh, P., Jarsjo, J., Kacergyte, I., Peacock, M., et al., 2023. Tradeoffs and synergies in wetland multifunctionality: a scaling issue. Sci. Total Environ. 862, 160746 https://doi.org/10.1016/j.scitotenv.2022.160746.

Haughton, N., Abramowitz, G., Pitman, A., Phipps, S.J., 2015. Weighting climate model ensembles for mean and variance estimates. Clim. Dyn. 45, 3169–3181. https://doi.org/10.1007/s00382-015-2531-3.

Hazeleger, W., Severijns, C., Semmler, T., Ştefănescu, S., Yang, S., Wang, X., et al., 2010. EC-Earth: a seamless earth-system prediction approach in action. Bull. Am. Meteorol. Soc. 91, 1357–1364.

Jacob, D., Teichmann, C., Sobolowski, S., Katragkou, E., Anders, I., Belda, M., et al., 2020. Regional climate downscaling over Europe: perspectives from the EURO-CORDEX community. Reg. Environ. Chang. 20, 1–20.

Jones, D.L., 2017. Fathom Toolbox for MATLAB: Software for Multivariate Ecological and Oceanographic Data Analysis. College of Marine Science, University of South Florida, St. Petersburg, FL, USA.

Jones, C., Hughes, J., Bellouin, N., Hardiman, S., Jones, G., Knight, J., et al., 2011. The HadGEM2-ES implementation of CMIP5 centennial simulations. Geosci. Model Dev. 4, 543–570.

Klöffel, T., Larsbo, M., Jarvis, N., Barron, J., 2024. Freeze-thaw effects on pore space and hydraulic properties of compacted soil and potential consequences with climate change. Soil Tillage Res. 239 https://doi.org/10.1016/j.still.2024.106041.

Knapp, J.L.A., Li, L., Musolff, A., 2022. Hydrologic connectivity and source heterogeneity control concentration–discharge relationships. Hydrol. Process. 36 https://doi.org/10.1002/hyp.14683.

Krysanova, V., Donnelly, C., Gelfan, A., Gerten, D., Arheimer, B., Hattermann, F., et al., 2018. How the performance of hydrological models relates to credibility of projections under climate change. Hydrol. Sci. J. 63, 696–720.

Krysanova, V., Hattermann, F.F., Kundzewicz, Z.W., 2020. How evaluation of hydrological models influences results of climate impact assessment—an editorial. Clim. Chang. 163, 1121–1141. https://doi.org/10.1007/s10584-020-02927-8.

Kyllmar, K., Forsberg, L.S., Andersson, S., Mårtensson, K., 2014. Small agricultural monitoring catchments in Sweden representing environmental impact. Agric. Ecosyst. Environ. 198, 25–35. https://doi.org/10.1016/j.agee.2014.05.016.

La Follette, P.T., Teuling, A.J., Addor, N., Clark, M., Jansen, K., Melsen, L.A., 2021. Numerical daemons of hydrological models are summoned by extreme precipitation. Hydrol. Earth Syst. Sci. 25, 5425–5446.

Li, L., Knapp, J.L.A., Lintern, A., Ng, G.H.C., Perdrial, J., Sullivan, P.L., et al., 2024. River water quality shaped by land–river connectivity in a changing climate. Nat. Clim. Chang. 14, 225–237. https://doi.org/10.1038/s41558-023-01923-x.

Lindström, G., Pers, C., Rosberg, J., Strömqvist, J., Arheimer, B., 2010. Development and testing of the HYPE (Hydrological Predictions for the Environment) water quality model for different spatial scales. Hydrol. Res. 41, 295. https://doi.org/10.2166/nh.2010.007.

Liu, J., Baulch, H.M., Macrae, M.L., Wilson, H.F., Elliott, J.A., Bergstrom, L., et al., 2019. Agricultural water quality in cold climates: processes, drivers, management options, and research needs. J. Environ. Qual. 48, 792–802. https://doi.org/10.2134/jeq2019.05.0220.

Mellander, P.E., Jordan, P., Bechmann, M., Fovet, O., Shore, M.M., McDonald, N.T., et al., 2018. Integrated climate-chemical indicators of diffuse pollution from land to water. Sci. Rep. 8, 944. https://doi.org/10.1038/s41598-018-19143-1.

Mellander, P.-E., Galloway, J., Hawtree, D., Jordan, P., 2022. Phosphorus mobilization and delivery estimated from long-term high frequency water quality and discharge data. Frontiers in Water 4. https://doi.org/10.3389/frwa.2022.917813.

Moriasi, D.N., Gitau, M.W., Pai, N., Daggupati, P., 2015. Hydrologic and water quality models: performance measures and evaluation criteria. Trans. ASABE 58, 1763–1785.

Mosley, L.M., 2015. Drought impacts on the water quality of freshwater systems; review and integration. Earth Sci. Rev. 140, 203–214. https://doi.org/10.1016/j.earscirev.2014.11.010.

Musolff, A., Schmidt, C., Selle, B., Fleckenstein, J.H., 2015. Catchment controls on solute export. Adv. Water Resour. 86, 133–146. https://doi.org/10.1016/j.advwatres.2015.09.026.

Nalbantis, I., Tsakiris, G., 2008. Assessment of hydrological drought revisited. Water Resour. Manag. 23, 881–897. https://doi.org/10.1007/s11269-008-9305-1.

Ockenden, M.C., Hollaway, M.J., Beven, K.J., Collins, A.L., Evans, R., Falloon, P.D., et al., 2017. Major agricultural changes required to mitigate phosphorus losses under climate change. Nat. Commun. 8, 161. https://doi.org/10.1038/s41467-017-00232-0.

Outram, F.N., Cooper, R.J., Sunnenberg, G., Hiscock, K.M., Lovett, A.A., 2016. Antecedent conditions, hydrological connectivity and anthropogenic inputs: factors affecting nitrate and phosphorus transfers to agricultural headwater streams. Sci. Total Environ. 545-546, 184–199. https://doi.org/10.1016/j.scitotenv.2015.12.025.

Payne, A.E., Demory, M.-E., Leung, L.R., Ramos, A.M., Shields, C.A., Rutz, J.J., et al., 2020. Responses and impacts of atmospheric rivers to climate change. Nature Reviews Earth & Environment 1, 143–157. https://doi.org/10.1038/s43017-020-0030-5.

Peterson, T.J., Saft, M., Peel, M.C., John, A., 2021. Watersheds may not recover from drought. Science 372, 745–749. https://doi.org/10.1126/science.abd5085.

Popke, D., Stevens, B., Voigt, A., 2013. Climate and climate change in a radiative-convective equilibrium version of ECHAM6. Journal of Advances in Modeling Earth Systems 5, 1–14.

R Core Team, 2022. R: a language and environment for statistical computing. In: R Foundation for Statistical Computing, editor. 4.1.3, Vienna, Austria.

Riml, J., Morén, I., Wörman, A., 2024. Potential of stream restorations to enhance the hyporheic removal of agricultural nitrogen in Sweden. Ecol. Eng. 201 https://doi.org/10.1016/j.ecoleng.2024.107194.

Rose, L.A., Karwan, D.L., Godsey, S.E., 2018. Concentration-discharge relationships describe solute and sediment mobilization, reaction, and transport at event and longer timescales. Hydrol. Process. 32, 2829–2844. https://doi.org/10.1002/hyp.13235.

Shamekh, S., Lamb, K.D., Huang, Y., Gentine, P., 2023. Implicit learning of convective organization explains precipitation stochasticity. Proc. Natl. Acad. Sci. U. S. A. 120, e2216158120 https://doi.org/10.1073/pnas.2216158120.

Shen, H., Tolson, B.A., Mai, J., 2022. Time to update the split-sample approach in hydrological model calibration. Water Resour. Res. 58 https://doi.org/10.1029/2021wr031523.

Stewart, B., Shanley, J.B., Kirchner, J.W., Norris, D., Adler, T., Bristol, C., et al., 2022. Streams as mirrors: reading subsurface water chemistry from stream chemistry. Water Resour. Res. 58 https://doi.org/10.1029/2021wr029931.

Strandberg, G., Bärring, L., Hansson, U., Jansson, C., Jones, C., Kjellström, E., et al., 2015. CORDEX Scenarios for Europe From the Rossby Centre Regional Climate Model RCA4. RMK 116. Swedish Meteorological and Hydrological Institute.

Strömqvist, J., Arheimer, B., Dahné, J., Donnelly, C., Lindström, G., 2012. Water and nutrient predictions in ungauged basins: set-up and evaluation of a model at the national scale. Hydrol. Sci. J. 57, 229–247. https://doi.org/10.1080/02626667.2011.637497.

Stutter, M.I., Graeber, D., Evans, C.D., Wade, A.J., Withers, P.J.A., 2018. Balancing macronutrient stoichiometry to alleviate eutrophication. Sci. Total Environ. 634, 439–447. https://doi.org/10.1016/j.scitotenv.2018.03.298.

Tebaldi, C., Knutti, R., 2007. The use of the multi-model ensemble in probabilistic climate projections. Philos Trans A Math Phys Eng Sci 365, 2053–2075. https://doi.org/10.1098/rsta.2007.2076.

The MathWorks Inc, 2022. MATLAB Version: 9.13.0 (R2022b). The MathWorks Inc., Natick, Massachusetts, United States.

Thompson, S.E., Basu, N.B., Lascurain, J., Aubeneau, A., Rao, P.S.C., 2011. Relative dominance of hydrologic versus biogeochemical factors on solute export across impact gradients. Water Resour. Res. 47 https://doi.org/10.1029/2010wr009605 (n/a-n/a).

Ulén, B., Stenberg, M., Wesström, I., 2016. Use of a flashiness index to predict phosphorus losses from subsurface drains on a Swedish farm with clay soils. J. Hydrol. 533, 581–590. https://doi.org/10.1016/j.jhydrol.2015.12.044.

Van Loon, A.F., Rangecroft, S., Coxon, G., Breña Naranjo, J.A., Van Ogtrop, F., Van Lanen, H.A.J., 2019. Using paired catchments to quantify the human influence on hydrological droughts. Hydrol. Earth Syst. Sci. 23, 1725–1739. https://doi.org/10.5194/hess-23-1725-2019.

van Meijgaard, E., Van Ulft, L., Van de Berg, W., Bosveld, F., Van den Hurk, B., Lenderink, G., et al., 2008. The KNMI Regional Atmospheric Climate Model RACMO, Version 2.1. KNMI De Bilt, The Netherlands.

Van Meter, K.J., Basu, N.B., Van Cappellen, P., 2017. Two centuries of nitrogen dynamics: legacy sources and sinks in the Mississippi and Susquehanna River Basins. Glob. Biogeochem. Cycles 31, 2–23. https://doi.org/10.1002/2016gb005498.

van Vliet, M.T.H., Thorslund, J., Strokal, M., Hofstra, N., Flörke, M., Ehalt Macedo, H., et al., 2023. Global river water quality under climate change and hydroclimatic extremes. Nature Reviews Earth & Environment 4, 687–702. https://doi.org/10.1038/s43017-023-00472-3.

Whitehead, P.G., Wilby, R.L., Battarbee, R.W., Kernan, M., Wade, A.J., 2009. A review of the potential impacts of climate change on surface water quality. Hydrol. Sci. J. 54, 101–123. https://doi.org/10.1623/hysj.54.1.101.

Winter, C., Lutz, S.R., Musolff, A., Kumar, R., Weber, M., Fleckenstein, J.H., 2021. Disentangling the impact of catchment heterogeneity on nitrate export dynamics from event to long-term time scales. Water Resour. Res. 57 https://doi.org/10.1029/2020wr027992.

Withers, P., Neal, C., Jarvie, H., Doody, D., 2014. Agriculture and eutrophication: where do we go from here? Sustainability 6, 5853–5875. https://doi.org/10.3390/su6095853.

Woodward, G., Bonada, N., Brown, L.E., Death, R.G., Durance, I., Gray, C., et al., 2016. The effects of climatic fluctuations and extreme events on running water ecosystems. Philos. Trans. R. Soc. Lond. Ser. B Biol. Sci. 371 https://doi.org/10.1098/rstb.2015.0274.

Wynants, M., Hallberg, L., Lindstrom, G., Strömqvist, J., M., B., 2024. How to achieve a 50% reduction in nutrient losses from agricultural catchments under different climate trajectories? Earth's Future. https://doi.org/10.1029/2023EF004299.

Yang, W., Andréasson, J., Graham, L.P., Olsson, J., Rosberg, J., Wetterhall, F., 2010. Distribution-based scaling to improve usability of regional climate model projections for hydrological climate change impacts studies. Hydrol. Res. 41, 211–229.